Planetary Companions to Evolved Intermediate-Mass Stars: 14 Andromedae, 81 Ceti, 6 Lyncis, and HD167042

Sato, Bun'ei ; Toyota, Eri ; Omiya, Masashi ; Izumiura, Hideyuki ; Kambe, Eiji ; Masuda, Seiji ; Takeda, Yoichi ; Itoh, Yoichi ; Ando,…

(Citation)
Publications of the Astronomical Society of Japan,60(6):1317-1326

(Issue Date)
2008-12-25

(Resource Type)
journal article

(Version)
Version of Record

(URL)
https://hdl.handle.net/20.500.14094/90001423

PASJ: Publ. Astron. Soc. Japan **60**, 1317–1326, 2008 December 25

Planetary Companions to Evolved Intermediate-Mass Stars: 14 Andromedae, 81 Ceti, 6 Lyncis, and HD 167042

Bun'ei SATO,[1] Eri TOYOTA,[2] Masashi OMIYA,[3] Hideyuki IZUMIURA,[4,5] Eiji KAMBE,[4] Seiji MASUDA,[6] Yoichi TAKEDA,[5,7] Yoichi ITOH,[2] Hiroyasu ANDO,[5,7] Michitoshi YOSHIDA,[4,5] Eiichiro KOKUBO,[5,7] and Shigeru IDA[8]

[1]*Global Edge Institute, Tokyo Institute of Technology, 2-12-1-S6-6 Ookayama, Meguro-ku, Tokyo 152-8550*
sato.b.aa@m.titech.ac.jp

[2]*Graduate School of Science, Kobe University, 1-1 Rokkodai, Nada, Kobe 657-8501*

[3]*Department of Physics, Tokai University, 1117 Kitakaname, Hiratsuka, Kanagawa 259-1292*

[4]*Okayama Astrophysical Observatory, National Astronomical Observatory of Japan, Kamogata, Okayama 719-0232*

[5]*The Graduate University for Advanced Studies, Shonan Village, Hayama, Kanagawa 240-0193*

[6]*Tokushima Science Museum, Asutamu Land Tokushima, 45-22 Kibigadani, Nato, Itano-cho, Itano-gun, Tokushima 779-0111*

[7]*National Astronomical Observatory of Japan, 2-21-1 Osawa, Mitaka, Tokyo 181-8588*

[8]*Department of Earth and Planetary Sciences, Tokyo Institute of Technology, 2-12-1 Ookayama, Meguro-ku, Tokyo 152-8551*

(Received 2008 May 6; accepted 2008 June 27)

Abstract

We report on the detection of four extrasolar planets orbiting evolved intermediate-mass stars from a precise Doppler survey of G–K giants at Okayama Astrophysical Observatory. All of the host stars are considered to be formerly early F-type or A-type dwarfs when they were on the main sequence. 14 And (K0 III) is a clump giant with a mass of $2.2\,M_\odot$ and has a planet of minimum mass $m_2 \sin i = 4.8\,M_{\rm J}$ in a nearly circular orbit with a 186 d period. This is one of the innermost planets around evolved intermediate-mass stars, and such planets have only been discovered in clump giants. 81 Cet (G5 III) is a clump giant with $2.4\,M_\odot$ hosting a planet of $m_2 \sin i = 5.3\,M_{\rm J}$ in a 953 d orbit with an eccentricity of $e = 0.21$. 6 Lyn (K0 IV) is a less-evolved subgiant with $1.7\,M_\odot$, and has a planet of $m_2 \sin i = 2.4\,M_{\rm J}$ in a 899 d orbit with $e = 0.13$. HD 167042 (K1 IV) is also a less-evolved star with $1.5\,M_\odot$ hosting a planet of $m_2 \sin i = 1.6\,M_{\rm J}$ in a 418 d orbit with $e = 0.10$. This planet was independently announced by Johnson et al. (2008, ApJ, 675, 784). All of the host stars have solar or sub-solar metallicity, which supports the lack of a metal-rich tendency in planet-harboring giants in contrast to the case of dwarfs.

Key words: stars: individual: 14 Andromedae — stars: individual: 81 Ceti — stars: individual: 6 Lyncis — stars: individual: HD 167042 — planetary systems — techniques: radial velocities

1. Introduction

Precise Doppler surveys of evolved stars have opened a new frontier in extrasolar planet searches during the past several years. Since successive discoveries of planets around K-type giants, ι Dra (Frink et al. 2002) and HD 47536 (Setiawan et al. 2003), and a G-type giant, HD 104985 (Sato et al. 2003), about 20 substellar companions orbiting evolved stars have been identified so far (Setiawan 2003; Setiawan et al. 2005; Sato et al. 2007, 2008; Hatzes et al. 2003, 2005, 2006; Reffert et al. 2006; Johnson et al. 2007a, 2008; Lovis & Mayor 2007; Niedzielski et al. 2007; Döllinger et al. 2007; Liu et al. 2008). Planets in evolved stars is now one of the major subjects in the field of extrasolar planets.

In the past, planets around evolved stars were primarily studied concerning the fate of our solar system, that is, whether the Earth and the other planets will be engulfed by the Sun in the future (Sackmann et al. 1993; Duncan & Lissauer 1998). On the other hand, the current Doppler surveys of evolved stars have been mainly carried out in the context of planet searches around intermediate-mass (1.5–5 $M_\odot$) stars. Intermediate-mass stars on the main sequence, that is early-type dwarfs (B–A dwarfs), are more difficult for Doppler planet searches because they have fewer absorption lines in their spectra than later type ones, which are often broadened due to their rapid rotation, and thus it is more difficult to achieve a high measurement precision in radial velocity that is sufficient to detect orbiting planets (but see e.g., Galland et al. 2005, 2006, which have developed a technique to extract Doppler information from spectra of A dwarfs sufficient for the detection of substellar companions). This is actually one of the major reasons why targets for planet searches had been limited to low-mass ($< 1.5\,M_\odot$) F–M dwarfs. On the contrary, late G to early K giants and subgiants, which are intermediate-mass stars in evolved stages, have many sharp absorption lines in their spectra appropriate for precise radial velocity measurements and their surface activity, such as pulsation, is quiet enough so as not to prevent us from detecting planets. Therefore, these types of stars have been identified as promising targets for Doppler planet searches around intermediate-mass stars.

The ongoing planet searches have already revealed that the properties of planets around evolved intermediate-mass stars are probably different from those around low-mass dwarfs (see Butler et al. 2006 or Udry & Santos 2007, and references therein for properties of planets around low-mass stars): 1) high frequency of massive planets (Lovis & Mayor 2007; Johnson et al. 2007b), which may be supported by the detection of a planet in an intermediate-mass giant in the Hyades

open cluster (Sato et al. 2007) despite the absence of planets in low-mass hundred dwarfs in the cluster (Paulson et al. 2004), 2) lack of inner planets with orbital semimajor axes of $\lesssim$0.7 AU (Johnson et al. 2007; Sato et al. 2008), and 3) lack of a metal-rich tendency in the host stars of planets (Pasquini et al. 2007; Takeda et al. 2008). Although these properties must reflect the history of the formation and evolution of planetary systems dependent on their host stars' mass, they are still in need of confirmation by a larger number of samples. Combined with such observational progress, planet-formation theories applicable to more massive stars than the Sun have begun to be developed rapidly (Ida & Lin 2005; Burkert & Ida 2007; Kennedy & Kenyon 2008) as an extension of the standard theory for solar-mass ones (e.g., Hayashi et al. 1985; Ida & Lin 2004) for the first time since Nakano (1988) explored the idea nearly 20 years ago.

In this paper, we report on the detection of four planets orbiting intermediate-mass G–K giants and subgiants (14 And, 81 Cet, 6 Lyn, and HD 167042) from the Okayama Planet Search Program (Sato et al. 2005), one of which (HD 167042) was independently announced by Johnson et al. (2008). We describe our observations in section 2. The properties of the host stars, radial-velocity data, and orbital parameters of their planets are presented in section 3. Section 4 is devoted to an analysis of the spectral line shape for the host stars. We summarize our results in section 5 along with a discussion about the properties of planets and host stars.

2. Observations

Since 2001, we have been conducting a precise Doppler survey of about 300 G–K giants (Sato et al. 2005) using a 1.88 m telescope, the HIgh Dispersion Echelle Spectrograph (HIDES: Izumiura 1999), and an iodine absorption cell (I_2 cell: Kambe et al. 2002) at Okayama Astrophysical Observatory (OAO). In 2007 December, HIDES was upgraded from a single CCD (2 K $\times$ 4 K) to a mosaic of three CCDs, which can simultaneously cover a wavelength range of 3750–7500 Å using a RED cross-disperser (Izumiura et al. in preparation). For precise radial velocity measurements, we used a wavelength range of 5000–5800 Å (covered by the middle CCD after the upgrade in 2007 December), in which many deep and sharp I_2 lines exist. The slit width was set to 200 μm (0.″76), giving a spectral resolution ($R = \lambda/\Delta\lambda$) of 67000 by about 3.3 pixels sampling. We can typically obtain a signal-to-noise ratio of S/N $>$ 200 pixel^{-1} for a $V < 6.5$ star with an exposure time shorter than 30 min. We achieved a long-term Doppler precision of about 6 m s^{-1} over a time span of 7 yr using our own analysis software for modeling an I_2-superposed stellar spectrum (Sato et al. 2002, 2005). Recently, we succeeded to attain a Doppler precision of about 2 m s^{-1} on a week-long time scale by improving the analysis software (Kambe et al. 2008). We are now trying to maintain the same precision on a year-long time scale.

For abundance analysis, we take a pure (I_2-free) stellar spectrum with the same wavelength range and spectral resolution as those for radial-velocity measurements. We also take a spectrum covering Ca II H K lines in order to check the chromospheric activity for stars showing large radial velocity variations. Although we can now take the spectrum simultaneously with radial-velocity data after the upgrade of HIDES, the spectra presented in this paper, except for HD 167042, were obtained before this upgrade. In that case, we set the wavelength range to 3800–4500 Å using a BLUE cross-disperser and a slit width of 250 μm, giving a wavelength resolution of 50000. We typically obtained S/N $\simeq$ 20 pixel^{-1} at the Ca II H K line cores for a $B = 6$ star with a 30 min exposure.

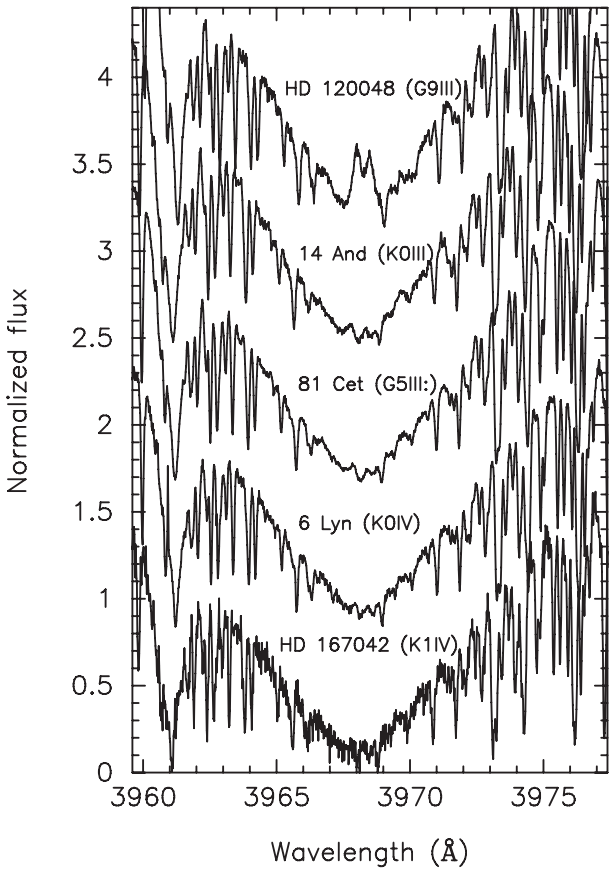

Fig. 1. Spectra in the region of Ca H lines. All of the planet-harboring stars show no significant emissions in line cores compared to that in the chromospheric active star HD 120048, which exhibits a velocity scatter of about 30 m s^{-1}. A vertical offset of about 0.7 has been added to each spectrum.

The reduction of echelle data (i.e., bias subtraction, flat-fielding, scattered-light subtraction, and spectrum extraction) is performed using the IRAF[1] software package in the standard way.

3. Stellar Properties, Radial Velocities, and Orbital Solutions

3.1. 14 Andromedae

14 And (HR 8930, HD 221345, HIP 116076) is listed in the Hipparcos catalog (ESA 1997) as a K0 III giant star with a V magnitude $V = 5.22$ and a color index $B - V = 1.029$.

[1] IRAF is distributed by the National Optical Astronomy Observatories, which is operated by the Association of Universities for Research in Astronomy, Inc. under cooperative agreement with the National Science Foundation, USA.

Table 1. Stellar parameters.*

Parameter	14 And	81 Cet	6 Lyn	HD 167042
Sp. Type	K0 III	G5 III:	K0 IV	K1 IV†
π (mas)	13.09 ± 0.71	10.29 ± 0.97	17.56 ± 0.76	20.00 ± 0.51
V	5.22	5.65	5.86	5.97
$B-V$	1.029	1.021	0.934	0.943
A_V	0.13	0.08	0.03	0.01
M_V	0.67	0.63	2.05	2.47
$B.C.$	−0.33	−0.34	−0.27	−0.28
$T_{\rm eff}$ (K)	4813 ± 20	4785 ± 25	4978 ± 18	4943 ± 12
$\log g$	2.63 ± 0.07	2.35 ± 0.08	3.16 ± 0.05	3.28 ± 0.05
v_t	1.43 ± 0.09	1.33 ± 0.06	1.10 ± 0.07	1.07 ± 0.07
[Fe/H]	-0.24 ± 0.03	-0.06 ± 0.03	-0.13 ± 0.02	$+0.00 \pm 0.02$
L ($L_\odot$)	58	60	15	10
R ($R_\odot$)	11 (10–12)	11 (10–13)	5.2 (4.9–5.6)	4.5 (4.3–4.7)
M ($M_\odot$)	2.2 (2.0–2.3)	2.4 (2.0–2.5)	1.7 (1.5–1.8)	1.5 (1.3–1.7)
$v \sin i$ (km s^{-1})	2.60	1.80	1.32	0.67

* The uncertainties of [Fe/H], $T_{\rm eff}$, $\log g$, and $v_{\rm t}$, are internal statistical errors (for a given data set of Fe I and Fe II line equivalent widths) evaluated by the procedure described in subsection 5.2 of Takeda et al. (2002). Since these parameter values are sensitive to slight changes in the equivalent widths as well as to the adopted set of lines (Takeda et al. 2008), realistic ambiguities may be by a factor of ∼2–3 larger than these estimates from a conservative point of view (e.g., 50–100 K in $T_{\rm eff}$, 0.1–0.2 dex in $\log g$). Values in the parenthesis for stellar radius and mass correspond to the range of the values assuming the realistic uncertainties in $\Delta \log L$ corresponding to parallax errors in the Hipparcos catalog, $\Delta \log T_{\rm eff}$ of ± 0.01 dex (∼ ± 100 K), and Δ[Fe/H] of ± 0.1 dex. The resulting mass value may also appreciably depend on the chosen set of theoretical evolutionary tracks (e.g., the systematic difference as large as $\sim 0.5\,M_\odot$ for the case of metal-poor tracks between Lejeune and Schaerer (2001) and Girardi et al. (2000); see also footnote 3 in Sato et al. 2008).

† The star is listed in the Hipparcos catalogue as a K1 III giant. But judged from the position of the star on the HR diagram (figure 2), the star should be better classified as a less evolved subgiant.

The Hipparcos parallax, $\pi = 13.09 \pm 0.71$ mas, corresponds to a distance of 76.4 ± 4.1 pc and an absolute magnitude of $M_V = 0.67$, taking into account a correction of the interstellar extinction, $A_V = 0.13$, based on Arenou et al's (1992) table. Hipparcos made a total of 80 observations of the star, revealing a photometric stability down to $\sigma = 0.006$ mag. Ca II H K lines of the star show no significant emission in the line cores, as shown in figure 1, suggesting that the star is chromospherically inactive.

We derived atmospheric parameters and the Fe abundance of ∼320 G–K giants, including all targets for the Okayama Planet Search Program based on a spectroscopic approach using the equivalent widths of well-behaved Fe I and Fe II lines (cf. Takeda et al. 2002 for a detailed description of this method; Takeda et al. 2008). For 14 And, $T_{\rm eff} = 4813$ K, $\log g = 2.63$ cm s^{-2}, $v_{\rm t} = 1.43$ km s^{-1}, and [Fe/H] = −0.24 were obtained. The bolometric correction was estimated to be B.C. = −0.33, based on Kurucz (1993)'s theoretical calculation. With the use of these parameters and theoretical evolutionary tracks of Lejeune and Schaerer (2001), we obtained the fundamental stellar parameters of $L = 58\,L_\odot$, $R = 11\,R_\odot$, and $M = 2.2\,M_\odot$, as summarized in table 1. The procedure described here is the same as that adopted by Takeda et al. (2005) [see subsection 3.2 of Takeda et al. (2005) and Note of table 1 for uncertainties involved in the stellar parameters]. The projected rotational velocity, $v \sin i = 2.60$ km s^{-1}, was also obtained by Takeda et al. (2008). Mishenina et al. (2006) obtained $T_{\rm eff} = 4664$ K (from line-depth-ratio analysis),

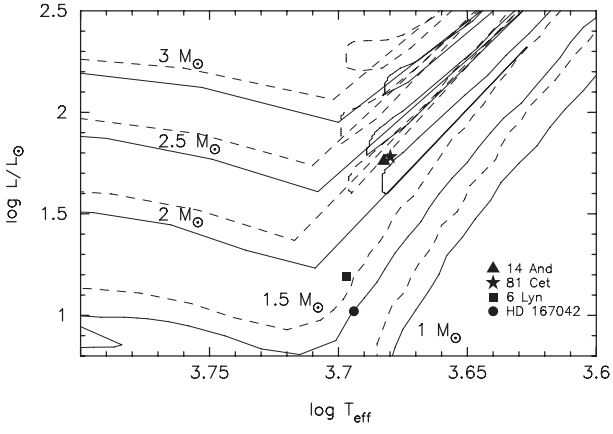

Fig. 2. HR diagram of the planet-harboring stars presented in this paper. Pairs of evolutionary tracks from Lejeune and Schaerer (2001) for stars with $Z = 0.02$ (solar metallicity; solid lines) and $Z = 0.008$ (dashed lines) of masses between 1 and $3\,M_\odot$ are also shown.

$\log g = 2.20$ cm s^{-2}, $v_{\rm t} = 1.4$ km s^{-1}, [Fe/H] = −0.37, and $M = 1.5\,M_\odot$ for the star. The temperature and [Fe/H] are by ∼150 K and by ∼0.1 dex lower than our estimates, respectively. Such differences can produce an $\sim 0.5\,M_\odot$ difference in the mass of a clump giant, especially for the metal-poor case, depending on the evolutionary models (see Note of table 1). As shown in figure 2, the star is located at the clump region on the HR diagram.

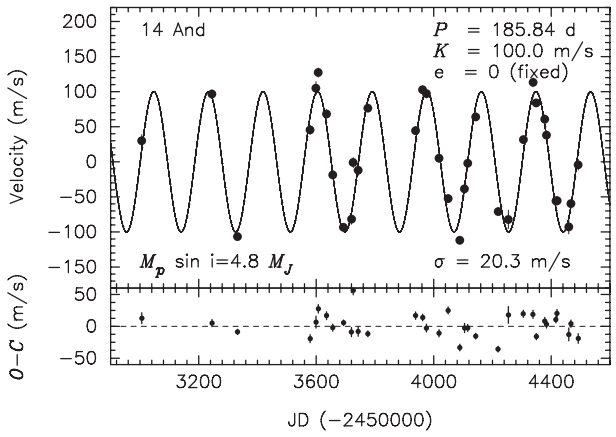

Fig. 3. Top: Observed radial velocities of 14 And (dots). A Keplerian orbital fit is shown by the solid line. Bottom: Residuals to the Keplerian fit. The rms to the fit is 20.3 m s^{-1}.

We collected a total of 34 radial velocity data of 14 And between 2004 January and 2008 January, with a typical S/N of 200 pixel^{-1} for an exposure time of about 600 s. The observed radial velocities are shown in figure 3 and are listed in table 2 together with their estimated uncertainties, which were derived from an ensemble of velocities from each of ~ 200 spectral regions (each 4–5 Å long) in every exposure. A Lomb–Scargle periodogram (Scargle 1982) of the data exhibits a dominant peak at a period of 188 d. To assess the significance of this periodicity, we estimated the False Alarm Probability (*FAP*), using a bootstrap randomization method in which the observed radial velocities were randomly redistributed, while keeping fixed the observation time. We generated 10^5 fake datasets in this way, and applied the same periodogram analysis to them. Since no fake datasets exhibited a periodogram power higher than the observed dataset, the *FAP* is less than 1×10^{-5}.

The observed radial velocities can be well-fitted by a circular orbit with a period of $P = 185.84 \pm 0.23$ d and a velocity semi-amplitude of $K_1 = 100.0 \pm 1.3$ m s^{-1}. The resulting model is shown in figure 3 overplotted on the velocities, and its parameters are listed in table 3. The uncertainty of each parameter was estimated using a Monte-Carlo approach. We generated 300 fake datasets by adding random Gaussian noise corresponding to velocity measurement errors to the observed radial velocities in each set, and then found the best-fit Keplerian parameters for each, and examined the distribution of each of the parameters. The rms scatter of the residuals to the Keplerian fit was 20.3 m s^{-1}, which is comparable those of giants with the same $B-V$ as 14 And in our sample (Sato et al. 2005). Adopting a stellar mass of 2.2 $M_\odot$, we obtained the minimum mass for the companion of $m_2 \sin i = 4.8\,M_{\rm J}$ and a semimajor axis of $a = 0.83$ AU. The planet is one of the innermost planets ever discovered around evolved stars.

3.2. 81 Ceti

81 Cet (HR 771, HD 16400, HIP 12247) is listed in the Hipparcos catalog (ESA 1997) as a G5 III: giant star with a V magnitude of $V = 5.65$, a color index of $B-V = 1.021$, and a parallax of $\pi = 10.29 \pm 0.97$ mas, corresponding to a distance of 97.2 ± 9.2 pc and an absolute magnitude of $M_V = 0.63$, corrected by the interstellar extinction, $A_V = 0.08$ (Arenou et al. 1992). Hipparcos made a total of 58 observations of the star, revealing a photometric stability down to $\sigma = 0.006$ mag. Ca II H K lines of the star show no significant emission in the line cores, as shown in the figure 1, suggesting that the star is chromospherically inactive. We derived fundamental stellar parameters for the star of $T_{\rm eff} = 4785$ K, $\log g = 2.35$ cm s^{-2}, $v_{\rm t} = 1.33$ km s^{-1}, [Fe/H] $= -0.06$, $L = 60\,L_\odot$, $R = 11\,R_\odot$, and $M = 2.4\,M_\odot$, as summarized in table 1. As shown in figure 2, the star is located at the clump region on the HR diagram. Mishenina et al. (2006) derived $T_{\rm eff} = 4840$ K (from line-depth-ratio analysis), $\log g = 2.50$ cm s^{-2}, $v_{\rm t} = 1.35$ km s^{-1}, [Fe/H] $= -0.01$, and $M = 2.5\,M_\odot$ for the star, which reasonably agrees with our estimates.

We collected a total of 33 radial-velocity data of 81 Cet between 2003 September and 2008 March, with a typical S/N of 200 pixel^{-1} for an exposure time of 900 s. The observed radial velocities are shown in figure 4, and are listed in table 4

Table 2. Radial velocities of 14 And.

JD (−2450000)	Radial velocity (m s^{-1})	Uncertainty (m s^{-1})
3005.9546	30.2	8.6
3245.2465	96.8	5.7
3332.0661	−106.7	4.0
3579.1759	45.6	6.2
3599.3078	104.9	9.3
3607.1357	127.2	6.6
3635.2106	68.1	6.2
3656.1741	−18.8	5.5
3693.0493	−93.2	4.3
3719.9577	−81.8	7.2
3726.0131	−1.1	7.0
3742.9362	−11.9	7.6
3775.9237	76.3	4.6
3938.2816	44.6	5.9
3962.2592	102.7	5.2
3975.1040	97.1	6.2
4018.0820	5.3	5.6
4049.1049	−52.6	5.5
4089.0127	−111.9	5.2
4104.8910	−38.6	7.3
4115.8872	−2.1	5.4
4142.9051	64.0	4.4
4219.2924	−70.8	4.6
4254.2487	−82.1	13.1
4305.1747	31.6	5.5
4338.1549	113.3	6.3
4349.1366	83.9	4.9
4378.1594	60.7	5.9
4384.0522	38.0	6.0
4415.9392	−55.8	5.0
4419.9316	−55.5	6.3
4460.0025	−92.7	10.1
4466.9496	−59.7	5.7
4491.8965	−4.1	7.6

Table 3. Orbital parameters.

Parameter	14 And	81 Cet	6 Lyn	HD 167042
P (d)	185.84 ± 0.23	952.7 ± 8.8	899 ± 19	417.6 ± 4.5
K_1 ($m\,s^{-1}$)	100.0 ± 1.3	62.8 ± 1.5	36.2 ± 1.7	33.3 ± 1.6
e	0 (fixed)	0.206 ± 0.029	0.134 ± 0.052	0.101 ± 0.066
ω (°)	0 (fixed)	175.0 ± 6.9	27 ± 27	82 ± 52
T_p (JD−2,450,000)	2861.4 ± 1.5	2486 ± 26	3309 ± 60	2974 ± 60
$a_1 \sin i$ (10^{-3} AU)	1.712 ± 0.024	5.39 ± 0.12	2.97 ± 0.16	1.274 ± 0.057
$f_1(m)$ ($10^{-6}\,M_\odot$)	1.936 ± 0.079	2.30 ± 0.15	0.431 ± 0.062	0.158 ± 0.022
$m_2 \sin i$ (M_J)	4.8	5.3	2.4	1.6
a (AU)	0.83	2.5	2.2	1.3
N_{obs}	34	33	30	29
rms ($m\,s^{-1}$)	20.3	9.2	10.6	8.0
Reduced $\sqrt{\chi^2}$	3.3	1.7	1.6	1.5

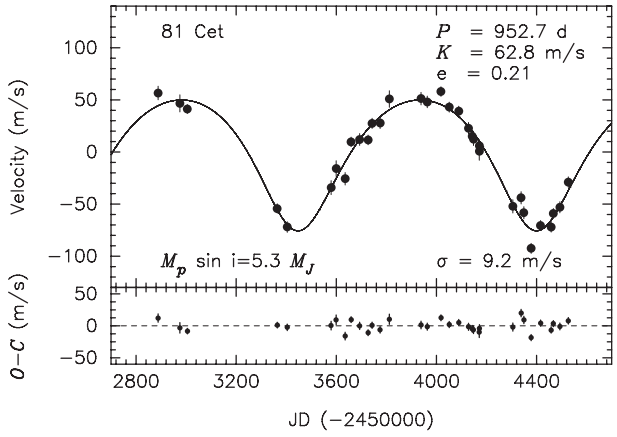

Fig. 4. Top: Observed radial velocities of 81 Cet (dots). The Keplerian orbital fit is shown by the solid line. Bottom: Residuals to the Keplerian fit. The rms to the fit is $9.2\,m\,s^{-1}$.

together with their estimated uncertainties. A Lomb–Scargle periodogram (Scargle 1982) of the data exhibits a dominant peak at a period of 983 d with a *FAP* value of $< 1 \times 10^{-5}$, which was estimated in the same way as described in subsection 3.1.

The observed radial velocities could be well-fitted by a Keplerian orbit with a period of $P = 952.7 \pm 8.8$ d, a velocity semiamplitude of $K_1 = 62.8 \pm 1.5\,m\,s^{-1}$, and an eccentricity of $e = 0.206 \pm 0.029$. The resulting model is shown in figure 4 overplotted on the velocities, and its parameters are listed in table 3. The uncertainty of each parameter was estimated using a Monte-Carlo approach, as described in subsection 3.1. The rms scatter of the residuals to the Keplerian fit is $9.2\,m\,s^{-1}$, which is small compared to the typical scatters of giants with the same $B - V$ as 81 Cet in our sample (Sato et al. 2005). Adopting a stellar mass of $2.4\,M_\odot$, we obtained a minimum mass for the companion of $m_2 \sin i = 5.3\,M_J$ and a semimajor axis of $a = 2.5$ AU. The planet is one of the outermost ones ever discovered around evolved stars.

3.3. 6 Lyncis

6 Lyn (HR 2331, HD 45410, HIP 31039) is a less-evolved K0 subgiant star with a V magnitude of $V = 5.86$, a color

Table 4. Radial velocities of 81 Cet.

JD (−2450000)	Radial velocity ($m\,s^{-1}$)	Uncertainty ($m\,s^{-1}$)
2888.2622	56.6	6.5
2975.1133	46.7	8.2
3005.0714	41.2	4.3
3364.0728	−54.2	4.5
3403.9822	−72.0	5.1
3579.2561	−34.2	6.8
3599.3232	−15.9	7.5
3635.2973	−25.7	6.0
3659.2479	9.7	4.6
3693.1606	12.0	5.7
3727.0642	11.6	4.7
3743.0368	27.4	4.9
3774.9443	27.7	5.2
3811.9192	50.8	8.0
3938.3038	51.2	6.0
3963.2839	48.1	5.6
4018.1630	58.0	4.6
4051.1382	43.0	4.8
4089.0958	39.1	4.8
4127.9761	22.8	5.5
4142.9929	15.1	5.3
4147.9770	12.3	6.0
4170.9343	0.7	8.7
4171.9188	6.0	5.9
4305.2794	−52.2	6.4
4338.2888	−44.0	5.9
4349.2596	−58.3	5.8
4378.1919	−92.5	4.8
4416.0384	−70.6	4.8
4458.0891	−72.1	4.8
4467.0517	−59.0	4.7
4493.0207	−53.1	5.4
4526.9147	−28.9	5.1

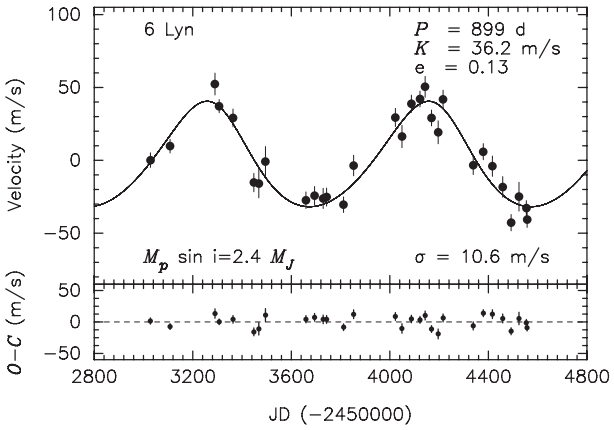

Fig. 5. Top: Observed radial velocities of 6 Lyn (dots). The Keplerian orbital fit is shown by the solid line. Bottom: Residuals to the Keplerian fit. The rms to the fit is 10.6 m s^{-1}.

index of $B-V=0.934$, and the Hipparcos parallax of $\pi=17.56\pm0.76$ mas (ESA 1997), placing the star at a distance of 56.9 ± 2.5 pc. The distance and an estimated interstellar extinction $A_V=0.03$ (Arenou et al. 1992) yield an absolute magnitude for the star of $M_V=2.05$. Hipparcos made a total of 73 observations of the star, revealing a photometric stability down to $\sigma=0.005$ mag. Ca II H K lines of the star show no significant emission in the line cores, as shown in the figure 1, suggesting that the star is chromospherically inactive. We derived fundamental stellar parameters for a star of $T_{\rm eff}=4978$ K, $\log g=3.16$ cm s^{-2}, $v_{\rm t}=1.10$ km s^{-1}, [Fe/H] $=-0.13$, $L=15\,L_\odot$, $R=5.2\,R_\odot$, and $M=1.7\,M_\odot$, as summarized in table 1. The position of the star on the HR diagram is plotted in figure 2 based on these parameters.

We collected a total of 30 radial velocity data of 6 Lyn between 2004 January and 2008 March, with a typical S/N of 200 pixel^{-1} for an exposure time of about 1200 s. The observed radial velocities are shown in figure 5, and are listed in table 5 together with their estimated uncertainties. A Lomb–Scargle periodogram (Scargle 1982) of the data exhibits a dominant peak at a period of 917 d with a *FAP* value of $<1\times10^{-5}$, which was estimated in the same way as described in subsection 3.1.

The observed radial velocities could be well-fitted by a Keplerian orbit with a period of $P=899\pm19$ d, a velocity semiamplitude of $K_1=36.2\pm1.7$ m s^{-1}, and an eccentricity of $e=0.134\pm0.052$. The resulting model is shown in figure 5, and its parameters are listed in table 3. The uncertainty of each parameter was estimated using a Monte-Carlo approach, as described in subsection 3.1. The rms scatter of the residuals to the Keplerian fit was 10.6 m s^{-1}, which is comparable to those for subgiants (Johnson et al. 2007). Adopting a stellar mass of $1.7\,M_\odot$, we obtained a minimum mass for the companion of $m_2\sin i=2.4\,M_{\rm J}$ and a semimajor axis of $a=2.2$ AU.

3.4. HD 167042

HD 167042 (HR 6817, HIP 89047) is classified in the Hipparcos catalog (ESA 1997) as a K1 III star with a V magnitude of $V=5.97$ and a color index of $B-V=0.943$. The Hipparcos parallax, $\pi=20.00\pm0.51$ mas, corresponds to a distance of 50.0 ± 1.3 pc and yields an absolute magnitude of $M_V=2.47$, corrected by interstellar extinction, $A_V=0.01$ (Arenou et al. 1992). Hipparcos made a total of 110 observations of the star, revealing a photometric stability down to $\sigma=0.007$ mag. Ca II H K lines of the star show no significant emission in the line cores, suggesting that the star is chromospherically inactive (figure 1). We derived fundamental stellar parameters for the star of $T_{\rm eff}=4943$ K, $\log g=3.28$ cm s^{-2}, $v_{\rm t}=1.07$ km s^{-1}, [Fe/H] $=+0.00$, $L=10\,L_\odot$, $R=4.5\,R_\odot$, and $M=1.5\,M_\odot$, as summarized in table 1. The position of the star on the HR diagram is plotted in figure 2 based on these parameters. Judged from the position, the star is considered to be a less evolved subgiant, like 6 Lyn, rather than a class III giant. Johnson et al. (2008) obtained $T_{\rm eff}=5010\pm75$ K, $\log g=3.47\pm0.08$ cm s^{-2}, [Fe/H] $=+0.05\pm0.06$, $M=1.64\pm0.13\,M_\odot$, $R=4.30\pm0.07\,R_\odot$, and $L=10.5\pm0.05\,L_\odot$ for the star, all of which well-agree with our estimates within the errors.

A planetary companion to HD 167042 was recently reported by Johnson et al. (2008). We collected a total of 29 radial-velocity data of the star between 2004 March and 2008 March, which is almost the same period of time as that of Johnson et al. The data have a typical S/N value of 200 pixel^{-1} for an

Table 5. Radial velocities of 6 Lyn.

JD (−2450000)	Radial velocity (m s^{-1})	Uncertainty (m s^{-1})
3028.2002	0.2	5.0
3107.9650	9.8	4.7
3290.2429	52.4	7.5
3307.1619	37.2	4.5
3363.3240	29.1	6.1
3448.0390	−15.3	6.3
3467.9581	−15.9	9.8
3494.9817	−0.8	10.3
3659.2879	−27.4	5.7
3694.3102	−24.2	6.2
3729.1980	−26.1	6.9
3743.1611	−25.2	6.2
3811.9435	−30.4	5.3
3852.9669	−3.6	7.1
4022.3010	29.4	6.2
4049.2443	16.4	7.7
4087.2793	38.8	6.0
4122.2054	42.1	5.5
4143.1678	50.4	7.2
4169.0485	29.1	5.5
4196.0062	19.2	7.9
4215.9689	41.8	6.3
4338.3163	−3.3	6.5
4379.2591	5.9	5.6
4416.1067	−4.0	7.0
4458.1686	−18.3	7.1
4492.1646	−42.8	5.6
4524.0101	−24.9	9.9
4553.9338	−32.8	5.2
4556.9840	−40.8	5.3

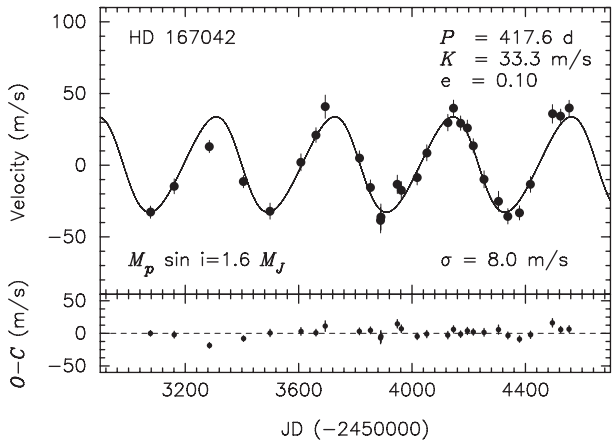

Fig. 6. Top: Observed radial velocities of HD 167042 (dots). The Keplerian orbital fit is shown by the solid line. Bottom: Residuals to the Keplerian fit. The rms to the fit is 8.0 m s^{-1}.

Table 6. Radial velocities of HD 167042.

JD (−2450000)	Radial velocity (m s^{-1})	Uncertainty (m s^{-1})
3077.3248	−32.8	4.3
3161.1350	−14.7	5.2
3285.0198	13.1	4.3
3405.3778	−11.5	4.3
3499.1405	−32.0	5.6
3608.0945	2.0	5.9
3661.0231	21.0	5.1
3693.9118	40.8	8.1
3814.3203	4.9	5.2
3853.2342	−15.4	5.2
3889.2354	−38.4	8.8
3890.1815	−36.1	9.1
3948.1031	−13.4	6.4
3962.1760	−17.4	6.0
4018.0037	−8.7	5.0
4051.9409	8.6	5.6
4126.3613	29.7	5.8
4146.3220	39.9	5.5
4171.2461	29.4	5.0
4195.2715	26.0	5.5
4216.2184	13.5	5.0
4254.1603	−9.9	5.9
4305.0598	−25.2	7.0
4338.0740	−35.6	5.3
4379.0062	−33.2	5.0
4417.8831	−13.4	5.5
4495.3581	35.8	6.5
4524.3108	34.3	4.9
4554.3268	39.9	5.4

exposure time of about 1500 s. The observed radial velocities are shown in figure 6, and are listed in table 6 together with their estimated uncertainties. A Lomb–Scargle periodogram (Scargle 1982) of the data exhibits a dominant peak at a period of 432 d with a *FAP* value of $< 1 \times 10^{-5}$, which was estimated in the same way as described in subsection 3.1.

The observed radial velocities can be well-fitted by a Keplerian orbit with a period of $P = 417.6 \pm 4.5$ d, a velocity semiamplitude of $K_1 = 33.3 \pm 1.6$ m s^{-1}, and an eccentricity of $e = 0.101 \pm 0.066$. The resulting model is shown in figure 6, and its parameters are listed in table 3. The uncertainty of each parameter was estimated using a Monte-Carlo approach, as described in subsection 3.1. The rms scatter of the residuals to the Keplerian fit was 8.0 m s^{-1}, which is consistent with the result of Johnson et al. (2008). Adopting a stellar mass of 1.5 $M_\odot$, we obtained a minimum mass for the companion of $m_2 \sin i = 1.6\,M_{\rm J}$ and a semimajor axis of $a = 1.3$ AU. All of the parameters are in good agreement with those obtained by Johnson et al. (2008), and thus we have independently confirmed the existence of the planet.

4. Line Shape Analysis

To investigate other causes producing apparent radial-velocity variations, such as pulsation and rotational modulation, rather than orbital motion, a spectral line-shape analysis was performed by using high-resolution stellar templates, followed by a technique of Sato et al. (2007). In our technique, we extracted a high-resolution iodine-free stellar template from several stellar spectra contaminated by iodine lines (Sato et al. 2002). The basic procedure of the technique was as follows: first, we modeled the observed star+I_2 spectrum in a standard manner, but using an initial guess of the intrinsic stellar template spectrum. Next, we took the difference between the observed star+I_2 spectrum and the modeled one. Since the difference is mainly considered to be due to an imperfection of the initial guess of the stellar template spectrum, we revised the initial guess, while taking account of the difference, and modeled the observed star+I_2 spectrum using a revised guess of the template. We repeated this process until we obtained sufficient agreement between the observed and modeled spectrum. We took average of the thus-obtained stellar templates from several observed star+I_2 spectra so as to increase the S/N ratio of the template. Details of this technique are described in Sato et al. (2002).

For a spectral line-shape analysis, we extracted two stellar templates from 5 star+I_2 spectra at the peak and valley phases of the observed radial velocities for each star. Then, cross-correlation profiles of the two templates were calculated for 50–80 spectral segments (4–5 Å width each) in which severely blended lines or broad lines were not included. Three bisector quantities were calculated for the cross-correlation profile of each segment: the velocity span (BVS), which is the velocity difference between two flux levels of the bisector; the velocity curvature (BVC), which is the difference of the velocity span of the upper half and the lower half of the bisector; and the velocity displacement (BVD), which is the average of the bisector at three different flux levels. We used flux levels of 25%, 50%, and 75% of the cross-correlation profile to calculate the above quantities. The resulting bisector quantities for each star are listed in table 7. As expected from the planetary hypothesis, both the BVS and the BVC for 81 Cet, 6 Lyn, and HD 167042 were identical to zero, which means that the

Table 7. Bisector quantities.

Bisector quantities	14 And	81 Cet	6 Lyn	HD 167042
Bisector Velocity Span (BVS) ($m\,s^{-1}$)	19.8 ± 5.8	2.4 ± 3.0	-5.5 ± 5.1	1.0 ± 4.3
Bisector Velocity Curve (BVC) ($m\,s^{-1}$)	-1.6 ± 2.8	-2.8 ± 2.1	-0.3 ± 4.1	1.9 ± 3.1
Bisector Velocity Displacement (BVD) ($m\,s^{-1}$)	-177.0 ± 11.2	-115.3 ± 7.4	-60.9 ± 8.9	-58.9 ± 8.0

cross-correlation profiles are symmetric, and the average BVD is consistent with the velocity difference between the two templates at the peak and valley phases of the observed radial velocities ($\simeq 2K_1$). The BVS for 14 And is about $20\,m\,s^{-1}$, which is large compared to those for other stars, suggesting a higher intrinsic variability and possible variations in the line profiles for the star. This may be consistent with the large rms scatters of the residuals to the Keplerian fit ($\sigma = 20.3\,m\,s^{-1}$) and higher rotational velocity ($v \sin i = 2.6\,km\,s^{-1}$) for the star. However, the BVD value ($-177\,m\,s^{-1}$) is consistent with the velocity difference between the two templates ($\simeq 2K_1$), and the BVS value is only about one ninth of the BVD. Thus, it is unlikely that the observed radial velocity variations are produced by changes in the line shape due to intrinsic activity, such as pulsation or rotational modulation.

Based on these results, we conclude that the radial velocity variability observed in these 4 stars are best explained by the orbital motion, although line-shape variability for 14 And deserves to be investigated in more detail.

5. Summary and Discussion

We have here reported on four new planets around evolved intermediate-mass stars observed from the Okayama Planet Search Program; two of them orbit clump giants and the other two orbit subgiants. In total, we have so far discovered 7 planets and 1 brown dwarf around intermediate-mass clump giants (2.1–2.7 $M_\odot$) and 2 planets around subgiants (1.5 and 1.7 $M_\odot$) in this program. The host stars are considered to be formerly early F-type or A-type dwarfs when they were on the main sequence.

Like all of the other planets found around these types of stars, the four planets presented in this paper reside beyond $\sim$0.7 AU from the central stars. Since many planets are known to exist within 0.7 AU around low-mass dwarfs, a lack of inner planets around evolved intermediate-mass stars must reflect a different history of formation and evolution of the planetary systems. Two scenarios can account for the orbital distribution: one is that inner planets are primordially deficient around intermediate-mass stars; the other is that they have been engulfed by the expanding central stars due to stellar evolution. Mass loss of the central star makes planets move outward because of their weakened gravitational pull on the planets, but any orbital change due to mass loss is negligible in the RGB phase for planets around intermediate-mass stars, because the mass loss of those stars in the RGB phase is negligible (see discussion in Sato et al. 2008). The lack of inner planets around less-evolved subgiants (Johnson et al. 2007, 2008) may favor the former scenario. Since there is no observational bias against detecting planets with small semimajor axes around subgiants, whose radii are $\sim 5 R_\odot$ ($= 0.025$ AU) at most, and their intrinsic variability in the radial velocity is adequately small ($\lesssim 10\,m\,s^{-1}$), a lack of inner planets around them may be primordial. On the other hand, as for planets around intermediate-mass clump giants, the evolutionary effect of the central stars can not be ignored. When we assume that many of the clump giants are post-RGB stars (core-helium-burning stars), planets in orbits with $\lesssim$0.5 AU could have been engulfed by the central stars at the tip of the RGB ($R_\star \sim 25$–$40 R_\odot$ for a 2–3 $M_\odot$ star) due to the tidal force from the central stars (Sato et al. 2008). Thus, we can not reject the possibility that planets had originally existed at short orbital distances around progenitors of clump giants. It should be noted that all of the four innermost planets around evolved intermediate-mass stars with semimajor axes of 0.7–1 AU have been discovered around clump giants. Excluding the planets around clump giants, all of the six planets ever discovered around intermediate-mass subgiants reside beyond 1 AU, which expands the lack of inner planets around them. Although the number is still small, the properties of planets might be different between the two populations when we consider that clump giants include $\gtrsim 2\,M_\odot$ stars while subgiants are limited up to $\lesssim 2 M_\odot$. A larger number of planets, which will be provided by ongoing Doppler surveys of evolved stars among the globe, enables us to derive their statistical properties more clearly.

All of the host stars of the four planets presented here have solar or sub-solar metallicity. The results support the lack of a metal-rich tendency in planet-harboring giants recently claimed by several authors (e.g., Pasquini et al. 2007; Takeda et al. 2008), which makes marked contrast to the case of dwarf stars, where planet-harboring stars tend to generally be metal-rich (see e.g., Gonzalez 2003 or Udry & Santos 2007, and references therein). An interpretation of the absence of metal-rich trend in planet-harboring giants still remains to be cleared. A high efficiency in core-accretion in massive proto-planetary disks around massive stars combined with a high efficiency in inward orbital migration of planets (finally falling into the central stars) in metal-rich disks might reproduce the lack of a metal-rich trend. Alternatively, a metallicity-independent planet formation scenario, such as a disk-instability model (e.g., Boss 2002), might be possible. Pasquini et al. (2007) pointed out a possibility that any metallicity excess in planet-harboring dwarfs originates from the accretion of metal-rich material, and that the excess is diluted by a deep convective envelope at the stage of giants. It should be noted, however, that there are no super-metal-rich stars with [Fe/H] $> +0.2$ in our sample, regardless of the existence of orbiting planets (Takeda et al. 2008). Since the frequency distribution of planets steeply rises in [Fe/H] $> +0.2$ for solar-type dwarfs (Fischer & Valenti 2005), we might see a metal-poor ([Fe/H] $< +0.2$)

tail of the same distribution, where the frequency of planets is less sensitive to metallicity, in the case of giants. A detailed investigation of the metallicity distribution for a population of giants is required to derive a firm conclusion concerning the planet-metallicity correlation in giants and its origin.

Host stars' metallicity could control the fate of orbiting planets as well as their birth. From the view point of the engulfment scenario, inner planets could be deficient around metal-rich clump giants of $\sim 2\,M_{\odot}$, compared to around metal-poor ones. A metal-rich star with $\sim 2\,M_{\odot}$ can have more than a two-times larger maximum radius ($> 70 R_{\odot}$) than a metal-poor one at the tip of RGB (cf. evolutionary tracks by Girardi et al. 2000; Lejeune & Schaerer 2001; Claret 2004, 2006, 2007), which may increase the chance for the central star to engulf the inner planets, even up to ~ 1 AU. However, the current knowledge about the evolutionary tracks of giants is not sufficient to estimate this effect precisely. The stellar evolutionary track at the RGB phase for a $\sim 2\,M_{\odot}$ star is sensitive to even a slight difference in the stellar mass and the metallicity, because this mass range is a border where helium-burning starts in a degenerated core or a non-degenerated one, and thus the tracks are largely dependent on the adopted models. To investigate the orbital distribution of planets around post-RGB stars, together with a precise determination of the stellar mass (by using technique of asteroseismology; e.g., Frandsen et al. 2002; Hatzes & Zechmeister 2007; Ando et al. 2008) and metallicity would conversely give constraints on the stellar evolution for this problematic mass range from the observational side.

As described above, recent discoveries of planets around evolved stars have made stellar evolution and the fate of planets a renewed area of study. This subject has been studied by several authors (Sackmann et al. 1993; Duncan & Lissauer 1998; Rasio et al. 1996; Siess & Livio 1999a,b; Villanver & Livio 2007), while mainly focusing on a solar-mass star based on interests in the future of the solar system, and/or an asymptotic giant branch star with the scope of planets in planetary nebula and white dwarfs. Siess and Livio (1999b) proposed that the IR excess and high Li abundance observed in a few percent of G–K giants originate from the accretion of a substellar companion. Now is the time to promote such kinds of studies more extensively, not only for solar-mass stars, but also for intermediate-mass ones, especially in the RGB phase by both theoretical and observational approaches.

This research is based on data collected at Okayama Astrophysical Observatory (OAO), which is operated by National Astronomical Observatory of Japan (NAOJ). We are grateful to all of the staff members of OAO for their support during the observations. Data analysis was in part carried out on an "sb" computer system operated by the Astronomy Data Center (ADC) and Subaru Telescope of NAOJ. We thank the National Institute of Information and Communications Technology for their support on a high-speed network connection for data transfer and analysis. B.S. is supported by MEXT's program "Promotion of Environmental Improvement for Independence of Young Researchers" under the Special Coordination Funds for Promoting Science and Technology. H.I. and M.Y. are supported by Grants-in-Aid for Scientific Research (C) No. 13640247 and (B) No. 18340055, respectively, from the Japan Society for the Promotion of Science (JSPS). This research has made use of the SIMBAD database, operated at CDS, Strasbourg, France.

References

Ando, H., Tan, K., Kambe, E., Sato, B., & Zhao, G. 2008, PASJ, 60, 219
Arenou, F., Grenon, M., & Gómez, A. 1992, A&A, 258, 104
Boss, A. P. 2002, ApJ, 567, L149
Burkert, A., & Ida, S. 2007, ApJ, 660, 845
Butler, R. P., et al. 2006, ApJ, 646, 505
Claret, A. 2007, A&A, 467, 1389
Claret, A. 2006, A&A, 453, 769
Claret, A. 2004, A&A, 424, 919
Döllinger, M. P., Hatzes, A. P., Pasquini, L., Guenther, E. W., Hartmann, M., Girardi, L., & Esposito, M. 2007, A&A, 472, 649
Duncan, M. J., & Lissauer, J. J. 1998, Icarus, 134, 303
ESA 1997, The Hipparcos and Tycho Catalogues, ESA SP-1200 (Noordwijk: ESA)
Fischer, D. A., & Valenti, J. 2005, ApJ, 622, 1102
Frink, S., Mitchell, D. S., Quirrenbach, A., Fischer, D. A., Marcy, G. W., & Butler, R. P. 2002, ApJ, 576, 478
Galland, F., Lagrange, A.-M., Udry, S., Chelli, A., Pepe, F., Beuzit, J.-L., & Mayor, M. 2005, A&A, 444, L21
Galland, F., Lagrange, A.-M., Udry, S., Beuzit, J.-L., Pepe, F., & Mayor, M. 2006, A&A, 452, 709
Girardi, L., Bressan, A., Bertelli, G., & Chiosi, C. 2000, A&AS, 141, 371
Gonzalez, G. 2003, Rev. Mod. Phys., 75, 101
Hatzes, A. P., Cochran, W. D., Endl, M., McArthur, B., Paulson, D. B., Walker, G. A. H., Campbell, B., & Yang, S. 2003, ApJ, 599, 1383
Hatzes, A. P., Guenther, E.W., Endl, M., Cochran, W. D., Döllinger, M.P., & Bedalov, A. 2005, A&A, 437, 743
Hatzes, A. P., et al. 2006, A&A, 457, 335
Hatzes, A. P., & Zechmeister, M. 2007, ApJ, 670, L37
Hayashi, C., Nakazawa, K., & Nakagawa, Y. 1985, in Protostars and planets II, ed. D. C. Black & M. S. Matthews (Tucson: University of Arizona Press), 1100
Ida, S., & Lin, D. N. C. 2004, ApJ, 604, 388
Ida, S., & Lin, D. N. C. 2005, ApJ, 626, 1045
Izumiura, H. 1999, in Proc. 4th East Asian Meeting on Astronomy, ed. P. S. Chen (Kunming: Yunnan Observatory), 77
Johnson, J. A., et al. 2007a, ApJ, 665, 785
Johnson, J. A., Butler, R. P., Marcy, G. W., Fischer, D. A., Vogt, S. S., Wright, J. T., & Peek, K. M. G. 2007b, ApJ, 670, 833
Johnson, J. A., Marcy, G. W., Fischer, D. A., Wright, J. T., Reffert, S., Kregenow, J. M., Williams, P. K. G., & Peek, K. M. G. 2008, ApJ, 675, 784
Kambe, E., et al. 2002, PASJ, 54, 865
Kambe, E., et al. 2008, PASJ, 60, 45
Kennedy, G. M., & Kenyon, S. J. 2008, ApJ, 673, 502
Kurucz, R. L. 1993, Kurucz CD-ROM, No. 13 (Harvard-Smithsonian Center for Astrophysics)

Lejeune, T., & Schaerer, D. 2001, A&A, 366, 538
Liu, Y.-J., et al. 2008, ApJ, 672, 553
Lovis, C., & Mayor, M. 2007, A&A, 472, 657
Mishenina, T. V., Bienaymé, O., Gorbaneva, T. I., Charbonnel, C., Soubiran, C., Korotin, S. A., & Kovtyukh, V. V. 2006, A&A, 456, 1109
Nakano, T. 1988, MNRAS, 230, 551
Niedzielski, A., et al. 2007, ApJ, 669, 1354
Pasquini, L., Döllinger, M. P., Weiss, A., Girardi, L., Chavero, C., Hatzes, A. P., da Silva, L., & Setiawan, J. 2007, A&A, 473, 979
Paulson, D. B., Cochran, W. D., & Hatzes, A. P. 2004, AJ, 127, 3579
Rasio, F. A., Tout, C. A., Lubow, S. H., & Livio, M. 1996, ApJ, 470, 1187
Reffert, S., Quirrenbach, A., Mitchell, D. S., Albrecht, S., Hekker, S., Fischer, D. A. Marcy, G. W., & Butler, R. P. 2006, ApJ, 652, 661
Sackmann, I. J., Boothroyd, A. I., & Kraemer, K. E. 1993, ApJ, 418, 457
Sato, B., et al. 2003, ApJ, 597, L157
Sato, B., Kambe, E., Takeda, Y., Izumiura, H., & Ando, H. 2002, PASJ, 54, 873
Sato, B., Kambe, E., Takeda, Y., Izumiura, H., Masuda, S., & Ando, H. 2005, PASJ, 57, 97
Sato, B., et al. 2007, ApJ, 661, 527
Sato, B., et al. 2008, PASJ, in press
Scargle, J. D. 1982, ApJ, 263, 835
Setiawan, J., et al. 2003, A&A, 398, L19
Setiawan, J. 2003, in Proc. Towards Other Earths, DARWIN/TPF and the Search for Extrasolar Terrestrial Planets, ed. M. Fridlund & T. Henning, compiled by H. Lacoste, ESA SP-539 (Noordwijk: ESA Publications Division), 595
Setiawan, J., et al. 2005, A&A, 437, L31
Siess, L., & Livio, M. 1999a, MNRAS, 304, 925
Siess, L., & Livio, M. 1999b, MNRAS, 308, 1133
Takeda, Y., Ohkubo, M., & Sadakane, K. 2002, PASJ, 54, 451
Takeda, Y., Sato, B., Kambe, E., Izumiura, H., Masuda, S., & Ando, H. 2005, PASJ, 57, 109
Takeda, Y., Sato, B., & Murata, D. 2008, PASJ, 60, 781
Udry, S., & Santos, N. C. 2007, ARA&A, 45, 397